

# Constructive Nanolithography and Nanochemistry: Local Probe Oxidation and Chemical Modification

Daan Wouters and Ulrich S. Schubert\*

Laboratory of Macromolecular Chemistry and Nanoscience, Center for Nanomaterials (cNM), Eindhoven University of Technology and Dutch Polymer Institute (DPI), P.O. Box 513, 5600 MB, Eindhoven, The Netherlands

Received April 27, 2003. In Final Form: August 8, 2003

The possibility to prepare and use submicrometer-sized patterns in successive functionalization reactions with quaternary ammonium salts and (functional) chlorosilanes, as well as cationic gold nanoparticles, is presented. Submicrometer-sized structures were prepared by local probe oxidation of octadecyl trichlorosilane functionalized silicon wafers. By this method, patterns were oxidized with 40-nm resolution, which can be used in local surface functionalization reactions. The principle of subsequent functionalization, either with additional quaternary ammonium salts or by a polymer grafting reaction, has been demonstrated.

## Introduction

In the current drive for miniaturization, lithographic techniques play an important role.<sup>1–4</sup> Techniques such as deep UV lithography<sup>4</sup> as well as electron- and particle-beam lithographies are gaining ground in applications for structural lithographic applications, such as experimental electrodes, and in the fabrication of complicated yet extremely small electronic circuits.<sup>3,5,6</sup> Simultaneously, scanning-probe-based patterning techniques have recently gained interest as a result of the wide applicability and relative ease of surface modification. Soon after the development of scanning tunneling microscopy (STM),<sup>7</sup> researchers have reported the possibility of using STM for surface patterning down to atomic resolution.<sup>8,9</sup> A number of examples have been reported in the literature,<sup>10</sup> but, unfortunately, only very few real-world applications are known up to now, which is mainly caused by the unavailability of suitable substrates. More stable, robust operation can be obtained by using atomic force microscopy (AFM) to pattern surfaces. Patterning of soft (polymer) surfaces can be done by local tip-induced surface damage<sup>11,12</sup> (by applying, for example, a high contact force). Recently, IBM has introduced a concept in which a polymer substrate is patterned by a heatable AFM tip.<sup>13–15</sup> In their “millipede” developments, high patterning speeds can be

obtained by the parallel operation of multiple single addressable tips (1024 tips in an array). Moreover, results of research toward the development of multiple-tip systems for dip-pen lithography have been reported. The usage of multiple-tip systems (increasing production speeds) may make the application of AFM-based techniques feasible in industrial applications.<sup>16,17</sup> AFM has also been reported to be able to pattern metallic and semiconducting surfaces by local oxidation processes by applying a bias voltage over a conductive tip and a sample (e.g., the oxidation of metallic titanium to slightly larger TiO<sub>2</sub>).<sup>18–21</sup> Although this patterning does not introduce any surface functionality, which is also the case for high-force and high-temperature patterning, the changes in height on the substrate may lead to applications in high-density data storage fields. Local functionality can be obtained when using probe-oxidation techniques on organic substrates.<sup>22–24</sup> On surfaces with an aliphatic nature, local oxidation leads to the formation of localized areas containing carboxylic end groups, thus changing the surface properties such as hydrophobicity and reactivity without affecting the surface roughness.<sup>23,24</sup> Local differences in polarity can be used in the adsorption of, for example, charged particles. Besides the change in polarity by the creation of carboxylic acid groups, these units can also be used in local chemical functionalization. In this contribution, the application of the latter two methods for the formation of functional submicrometer “devices”, using conductive AFM as a

\* Author to whom correspondence should be addressed. Fax: (+31) 40-247-4186. E-mail: u.s.schubert@tue.nl.

(1) Schmidt, O. G.; Deneke, Ch.; Nakamura, Y.; Zapf-Gottwick, R.; Mueller, C.; Jin-Phillipp, N. Y. *Adv. Solid State Phys.* **2002**, *42*, 231.

(2) Service, R. F. *Science* **2002**, *298*, 2322.

(3) Service, R. F. *Science* **2001**, *293*, 782.

(4) Ito, T.; Okazaki, S. *Nature* **2000**, *406*, 1027.

(5) Langford, R. M.; Petford-Long, A. K.; Rommeswinkle, M.; Egelkamp, S. *Mater. Sci. Technol.* **2002**, *18*, 743.

(6) Horstmann, J. T.; Gosler, K. F. *Microelectron. Eng.* **2002**, *61–62*, 601.

(7) Binnig, G.; Rohrer, H.; Gerber, Ch.; Weibel, E. *Phys. Rev. Lett.* **1982**, *49*, 57.

(8) Demir, U.; Balasubramanian, K. K.; Cammarata, V.; Shannon, C. *J. Vac. Sci. Technol., B* **1996**, *13*, 1294.

(9) Schoer, J. K.; Zamborini, F. P.; Crooks, R. M. *J. Phys. Chem.* **1996**, *100*, 11086.

(10) Heinrich, A. J.; Lutz, C. P.; Gupta, J. A.; Eigler, D. M. *Science* **2002**, *298*, 1381.

(11) Klehn, B.; Kunze, U. *J. Appl. Phys.* **1999**, *85*, 3897.

(12) Heyde, M.; Rademann, K.; Cappella, B.; Geuss, M.; Sturm, H.; Spangenberg, T.; Niehus, H. *Rev. Sci. Instrum.* **2001**, *72*, 136.

(13) Vettiger, P.; Brugger, J.; Despont, M.; Drechsler, U.; Durig, U.; Haberle, W.; Lutwyche, M.; Rothuizen, H.; Stutz, R.; Widmer, R.; Binnig, G. *Microelectron. Eng.* **1999**, *46*, 11.

(14) Vettiger, P.; Despont, M.; Drechsler, U.; Durig, U.; Haberle, W.; Lutwyche, M. I.; Rothuizen, H. E.; Stutz, R.; Widmer, R.; Binnig, G. K. *IBM J. Res. Dev.* **2000**, *44*, 323.

(15) Durig, U.; Cross, G.; Despont, M.; Drechsler, U.; Haberle, W.; Lutwyche, M. I.; Rothuizen, H.; Stutz, R.; Widmer, R.; Vettiger, P.; Binnig, G. K.; King, W. P.; Goodson, K. E. *Tribol. Lett.* **2000**, *9*, 25.

(16) Hong, S.; Mirkin, C. A. *Science* **2000**, *288*, 1808.

(17) Hong, S.; Zhu, J.; Mirkin, C. A. *Science* **1999**, *286*, 523.

(18) Lemesko, S.; Gavrilov, S.; Shevyakov, V.; Roschin, V.; Solomatenko, R. *Nanotechnology* **2001**, *12*, 273.

(19) Campbell, P. M.; Snow, E. S.; McMarr, P. J. *Appl. Phys. Lett.* **1993**, *63*, 749.

(20) Kramer, N.; Birk, H.; Jorritsma, J.; Schönenberger, C. *Appl. Phys. Lett.* **1995**, *66*, 1325.

(21) Sugimura, H.; Nakagiri, N. *Jpn. J. Appl. Phys.* **1995**, *34*, 3406.

(22) Chien, F. S.-S.; Hsieh, W.-F.; Gwo, S.; Vladar, A. E.; Dagata, J. A. *J. Appl. Phys.* **2002**, *91*, 10044.

(23) Maoz, R.; Cohen, S. R.; Sagiv, J. *Adv. Mater.* **1999**, *11*, 55.

(24) Maoz, R.; Frydman, E.; Cohen, S. R.; Sagiv, J. *Adv. Mater.* **2000**, *12*, 424.

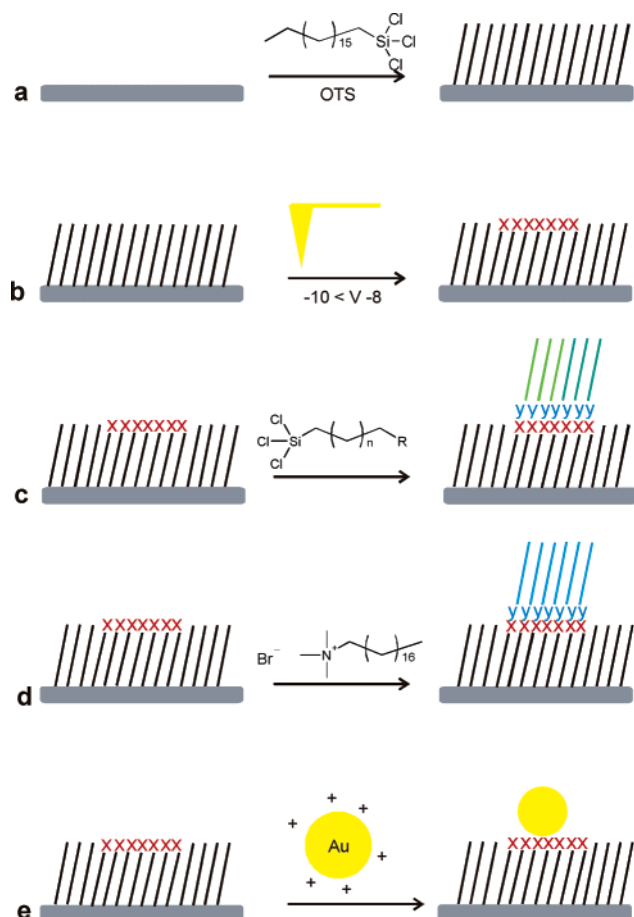


**Figure 1.** Schematic representation of the oxidation and functionalization of OTS-passivated silicon wafers. (a) Preparation of OTS passivated silicon wafers, (b) local probe oxidation of the OTS-functionalized wafers, (c) reaction of chlorosilanes to the oxidized patterns created in step b; 1,  $n = 16$ ,  $R = \text{CH}_3$ ; 2,  $n = 9$ ,  $R = -\text{CH}_2 = \text{CH}_2$ , (d) coupling of quaternary ammonium salts to the oxidized patterns, and (e) adsorption of positively charged gold nanoparticles to the pattern.

surface patterning tool and subsequent specific adsorption and chemical functionalization, are described.

## Results and Discussion

With the use of a conductive AFM tip, the production and chemical modification of submicrometer-sized functional structures were performed. The experimental procedure is represented schematically in Figure 1, which will be used throughout the text to clarify specific steps and to address results.

**a. Patterning of the Surface.** The bases for all the functionalization experiments were silicon wafers that were functionalized with octadecyl trichlorosilane (OTS). Chlorosilanes were chosen because they are well-known compounds used in surface-modification reactions with surface hydroxyl groups. OTS was selected because of its widespread availability and the presence of extensive experimental data.<sup>25,26</sup> In the present paper, functionalization of the wafers was performed in bis(cyclohexane) (BCH) as the solvent, which resulted in the formation of apolar flat substrates. The functionalization of the wafers with OTS was investigated by contact-angle measurements. The contact angle between water and a fully functionalized wafer should be  $110$ – $115^\circ$ .<sup>25,26</sup> The observed average contact angle (for three experiments) for the wafer was  $103.1^\circ$  after a 2-min and  $111.0^\circ$  after a 5-min reaction time, indicating full functionalization after 5 min.<sup>25,26</sup>

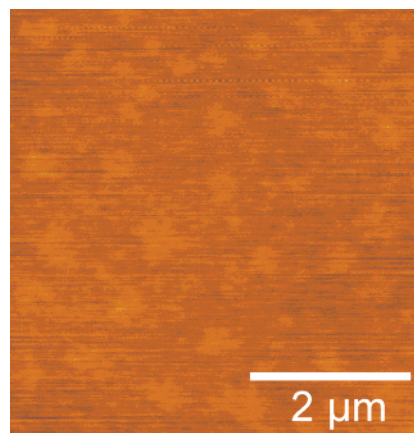


**Figure 2.** AFM height image ( $5.25 \times 5.25 \mu\text{m}$ ) of an OTS-functionalized wafer. Image was recorded in tapping mode ( $z$  range =  $1.0 \text{ nm}$ ). Domains of horizontally polymerized OTS embedded in a disordered matrix of covalently attached OTS are visible.

Monochlorosilanes as well as silanes with varying chain lengths and end groups should also work, but currently no attempts have been made in this direction.

The surface-functionalized wafers were examined with AFM (see Figure 2). The presence of  $200$ – $1000$ -nm-sized domains on the surface indicated islands of horizontally polymerized OTS in a matrix of more randomly attached chains. The height difference between these areas, however, is negligible, and no differences in properties have been encountered. However, experiments in which the functionalization was performed in toluene containing 1 equiv of water resulted only in horizontally polymerized domains. Unfortunately, they grew with time but never reached sizes that are suitable for patterning experiments. The role of (residual) water in the monolayer formation is extremely important, and more details on processes involving the horizontal and vertical polymerization of OTS with water can be found in the literature.<sup>25</sup>

**b. Local Probe Oxidation.** Local probe oxidation was carried out by applying a negative bias voltage ( $-8$  to  $-10 \text{ V}$ ) to a  $\text{W}_2\text{C}$ -coated AFM tip while moving the tip, in the contact mode, over the OTS-covered surface of a wafer along a user-defineable pattern. Upon oxidation (conversion of terminal methyl groups to carboxylic acids),<sup>21,22</sup> the height remained nearly constant, but an increase in the lateral friction signal indicated successful oxidation because the oxidized (more polar) areas have increased interaction with the tip and, therefore, increased friction (see Figure 3). Note also that upon prolonged oxidation the OTS self-assembled monolayer will be completely oxidized and that anodization of the silicon oxide substrate will take place.<sup>27</sup> The observed line widths in the results shown in Figure 3 were  $70 \text{ nm}$ . However, obtainable line widths depend strongly on the relative humidity, applied bias voltage, and contact force, as well as the contact time and in particular the tip shape and conductivity. A resolution down to  $20 \text{ nm}$  seems to be possible. Oxidation was carried out in the “vector mode” at  $3000 \text{ nm/s}$ , resulting in a typical total oxidation time of  $5 \text{ s}$ . In this mode, a pathway for the tip was drawn using vectors. A bitmap template image can also be utilized, but in that case oxidation parameters will be determined for each pixel in

(25) Fadeev, A. Y.; McCarthy, T. J. *Langmuir* **2000**, *16*, 7268.

(26) Kitaev, V.; Seo, M.; McGovern, M. E.; Huang, Y.-J.; Kumachev, E. *Langmuir* **2001**, *17*, 4274.

(27) Ahn, S. J.; Jang, Y. K.; Lee, H.; Lee, H. *Appl. Phys. Lett.* **2002**, *80*, 2592.

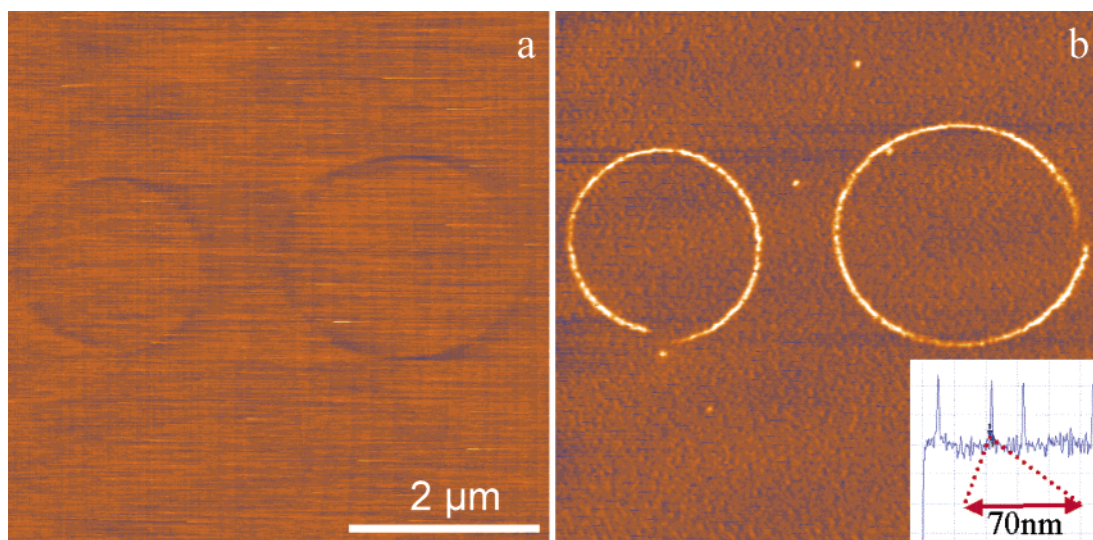


**Figure 3.** (a) Height image ( $4 \times 4 \mu\text{m}$ ) of the surface patterned by oxidizing to circles in the vector-drawing mode. The height of the surface is only slightly affected; oxidized areas are  $\sim 0.2\text{-nm}$  lower ( $z$  range =  $2\text{ nm}$ ). (b) Lateral-force image of the same area. The oxidized features are clearly visible. The line width in this example is  $70\text{ nm}$ , indicated by the line scan across the center of the image. In the text, the results of several different functionalization strategies are described.

the image, resulting in a very low overall speed. Depending on the tip and relative humidity, the oxidation speed may be increased up to  $3300\text{ nm/s}$ . In the case that the oxidation is carried out at too-high voltages or for too-long times, a decreasing height profile induced by partial oxidation of the OTS chains (probably degradation to  $\text{CO}_2$ ) is observed.

**c. Reaction with Chlorosilanes.** The oxidized patterns were used for coupling reactions with two chlorosilanes: OTS and 11-undecyl trichlorosilane (UTS). When these reactions were performed with, for example, OTS, a clear observable change in the height profile was observed. Results for two different templates are shown in Figure 4. In the first example (top four images), two spots ( $d = 200\text{ nm}$ ) and, in the second example (bottom four images), a line (width =  $160\text{ nm}$ ) were used as templates.

Successful functionalization of the oxidized patterns with OTS is indicated by the observed change in height. Comparing the oxidized patterns (Figure 4 a,e) with the OTS-functionalized patterns (Figure 4 c,g) showed a height increase by  $6\text{ nm}$  due to the attachment of  $10\text{--}50\text{-nm}$ -sized spherical domains to the surface. The change in height is more than expected from the attachment of a single monolayer, and the observation of  $10\text{--}50\text{-nm}$ -sized spherical domains indicates that both the covalent attachment of OTS to the oxidized substrate and the polymerization of OTS with surface-bound water took place. The prepared surface functionalities could also be reacted with functional chlorosilanes, thus introducing local (chemical) functionality. For this purpose, UTS was selected, which allowed both a direct functionalization of the terminal vinyl group and the radical copolymerizations. For the latter purpose, two samples have been prepared: in the first one, the pattern was reacted only with UTS (see next section), and in the second case, UTS was diluted with 10 equiv of OTS to isolate the terminal vinyl functionalities (see Figure 5).

Figure 5 demonstrates the successful formation of several  $100 \times 200\text{-nm}$ -sized OTS/UTS-functionalized islands with  $200\text{--}500\text{-nm}$  spacing. The attachment of chlorosilanes is indicated by a change in height of  $5\text{ nm}$ . Again, the presence of spherical domains on the pattern, with their height greater than that of a monolayer, indicate (co)polymerization of the chlorosilane functionalities with

surface-bound water. For the selective formation of monolayers, the amount of surface water present and the utilized reaction time should be reduced.

**Coupling of Polystyrene.** The coupling of polymers to the vinyl-functionalized pattern was attempted by exposing the wafer to a radical polymerization of styrene. After the reaction, the surface was thoroughly rinsed with toluene and water and cleaned with adhesive tape. Subsequently, the surface was examined by tapping-mode AFM (Figure 6).

Only in very selected spots was a change in the height profile detected, indicating that only a small amount of polymer chains were attached to the pattern. The low degree of coupling is probably due to the ability of the UTS-functionalized patterns for horizontal polymerization (thus removing all available terminal vinyl groups without causing a detectable change in height). However, the polymers that were attached were bound very tightly. They could not be removed by rinsing or cleaning with adhesive tape, nor by repeated contact-mode AFM scanning. Polymer grafting experiments on substrates functionalized with isolated single-site UTS should provide better results because of the reduced possibility for horizontal polymerization. Such approaches are currently under investigation.

**d. Adsorption of Quaternary Ammonium Salts.** Figure 7 shows a schematic representation of the sequential adsorption of trimethyloctadecylammonium bromide (TOA) to an oxidized template. In the first step, an area was oxidized using the previously mentioned procedure (see section a). In the second step, the surface was functionalized by exposing the surface to a water solution of TOA. The resulting adsorbed layer was imaged, and the complete procedure was repeated for three cycles.

Figure 8 shows the details of this procedure for the first cycle. In the top images (a and b), the oxidized area is shown. This pattern was obtained by loading a bitmap image of a gate and oxidizing the bright pixels in the image only. This is in contrast to the other experiments where the structures were created using the "vector" mode. Figure 8a shows a height image made by contact-mode AFM; the oxidation procedure has nearly no effect on the height profile of the sample, and only  $0.2\text{-nm}$  differences were observed. In Figure 8b, the corresponding lateral-

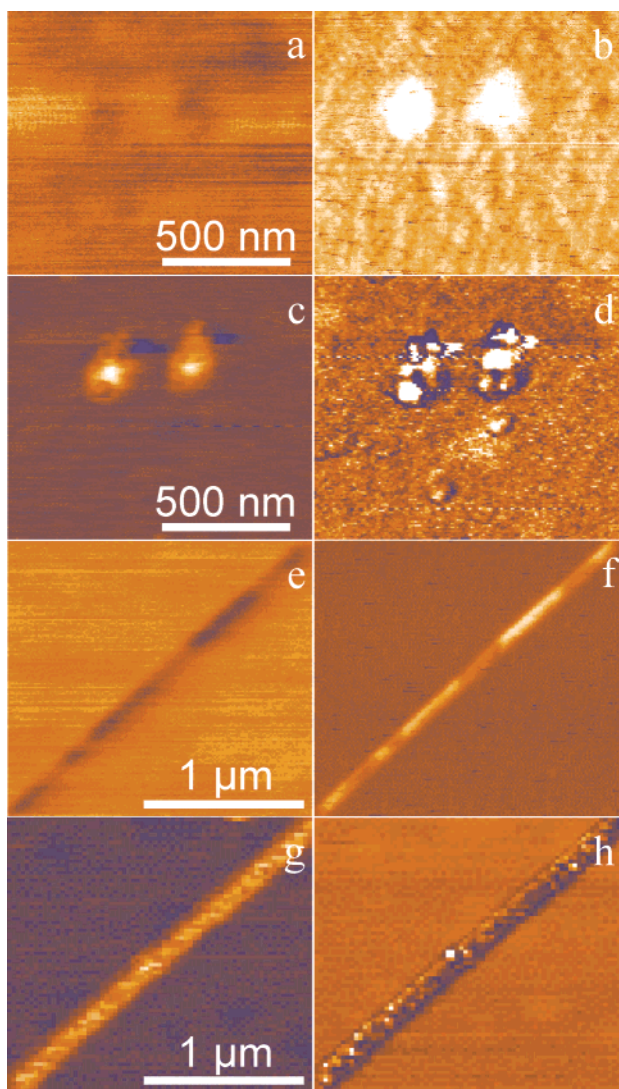


**Figure 4.** Two examples of OTS reacted with a probe-oxidized template. (a) Height image ( $z$  range = 0.5 nm) of the first example of an oxidized template, (b) corresponding lateral-force image of the template, (c) height image ( $z$  range = 6 nm) of the template area after the reaction with OTS, (d) corresponding phase image after the reaction with OTS, (e) height image ( $z$  range = 0.5 nm) of the second example with a different probe-oxidized template, (f) corresponding lateral-force image of the second template, (g) height image ( $z$  range = 6 nm) of the second template area after the reaction with OTS, and (h) corresponding phase images of the second-template area reaction with OTS.

force (friction) image is shown, which clearly demonstrates the effect of the oxidation: the oxidized, more-polar areas have increased interaction with the tip and, therefore, increased friction can be observed. Upon adsorption of the ammonium salt, the observation reverses: the height increases by about 2.0 nm (Figure 8c), which corresponds to the length of the C18 chain of the TOA. Moreover, the friction signal (Figure 8d) is reduced because of the fact that now the surface of the oxidized area, like that in the unoxidized parts, is dominated by the apolar methyl end groups of the C18 chains of TOA and, respectively, OTS.

Figure 9 shows the result of a sequential oxidation/functionalization with quaternary ammonium salts (see Figure 7 for a schematic presentation of one cycle). A total number of six steps (three cycles) were required to obtain the structure shown. The left image displays a contact-mode height image ( $30 \times 30 \mu\text{m}$ ,  $z$  range = 2.0 nm) of the results after five steps. Step 1 was the oxidation of the

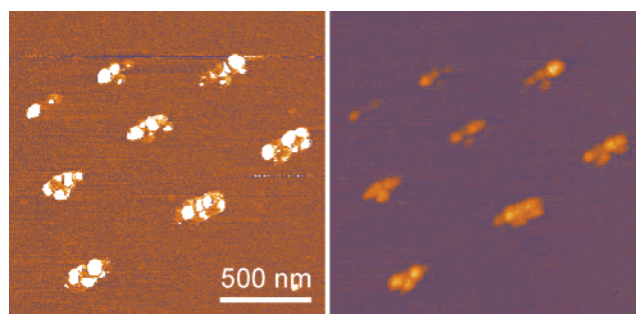


**Figure 5.** Left: tapping-mode height image of the surface ( $1.75 \times 1.75 \mu\text{m}$ ) with a 10:1 mixture of OTS and UTS reacted to a template ( $z$  range = 5 nm). Right: phase image of the left picture. Image shows the formation of “islands” of polymerized silanes attached to the substrate.

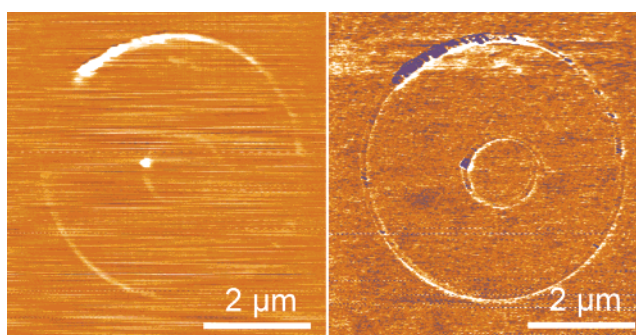


**Figure 6.** Left: tapping-mode height image of the surface ( $6 \times 6 \mu\text{m}$ ) after polymerization ( $z$  range = 20 nm). Right: phase image of the surface ( $6 \times 6 \mu\text{m}$ ). Functionalization is in complete.

star shape marked “a”. Step 2 was the adhesion of TOA to “a”, which resulted in an observed change in height along the pattern of 1.5 nm (see inset), indicating the addition of one monolayer of TOA to the oxidized pattern. Step 3 involved the oxidation of the triangle marked “b”. In step 4, the adhesion of TOA to “b” was confirmed by an observed height change of 1.5 nm. In step 5, the start of the third cycle, the oxidation of the shape marked “c” was done. The observed change in height for the oxidation is 0.2 nm (indicated by the inset). The right image displays a contact mode height image of the results after completion of the sixth step, which is the addition of TOA to the area marked “c”. The adsorption of TOA to area “c” again increased the observed height by approximately 1.5 nm, corresponding to the addition of one layer of TOA. Between cycles, the surfaces were washed with water. Assembled layers from the previous steps remained intact upon oxidation and also upon adsorption of additional salts.

**e. Adsorption of Gold Nanoparticles.** Much like the adsorption of positively charged molecules, gold nanoparticles can also be adsorbed onto the patterned surface. Because gold nanoparticles commonly have a negative surface charge due to stabilization with citric acid, they cannot be used directly. However, cationic gold nanoparticles having a coating of poly-L-lysine can be utilized. The results of an experiment in which cationic gold nanoparticles with a diameter of 20 nm were adsorbed onto a pattern can be seen in Figure 10. In the tapping-mode image, the particles can be observed clearly as 18–20-nm-high spots aligned on the oxidized pattern. However, the patterns are not completely covered by gold nanoparticles. In the areas between the particles, a region with a height of approximately 6 nm is observed, which is ascribed to the adsorption of free poly-L-lysine chains from the cationic gold particles solution. The successful

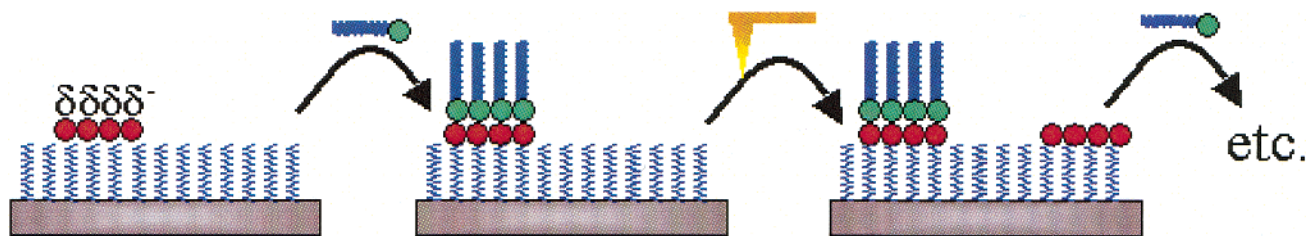


**Figure 7.** Schematic representation of the sequential addition of ammonium salts to oxidized patterns.

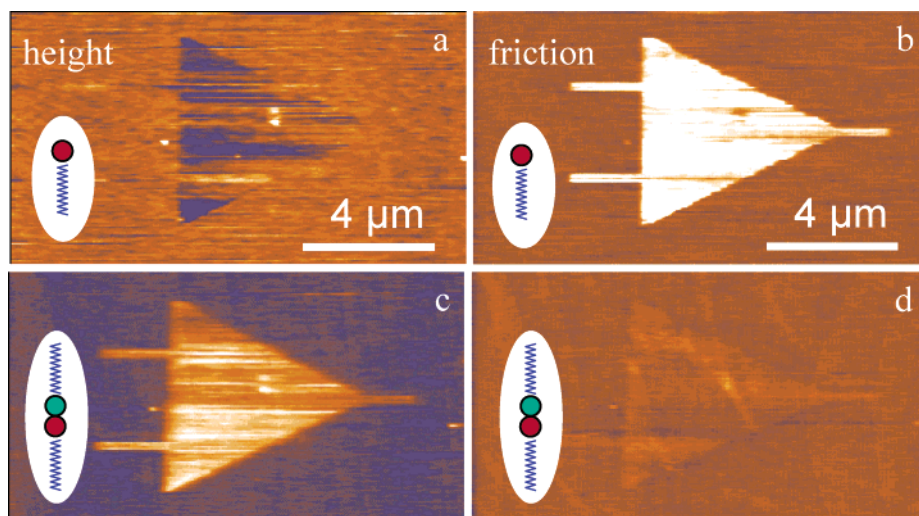


**Figure 8.** (a) Contact model height image ( $8 \times 14 \mu\text{m}$ ,  $z$  range = 0.5 nm) of an oxidized triangle. (b) Friction image belonging to the top-right image, indicating successful oxidization of the triangular shape. (c) Height image after ( $8 \times 14 \mu\text{m}$ ,  $z$  range = 0.5 nm) exposing the surface to a water solution of TOA, causing the height of the area to increase by 2.0 nm, indicating the adsorption of one layer of TOA. (d) Friction image belonging to bottom-left image.

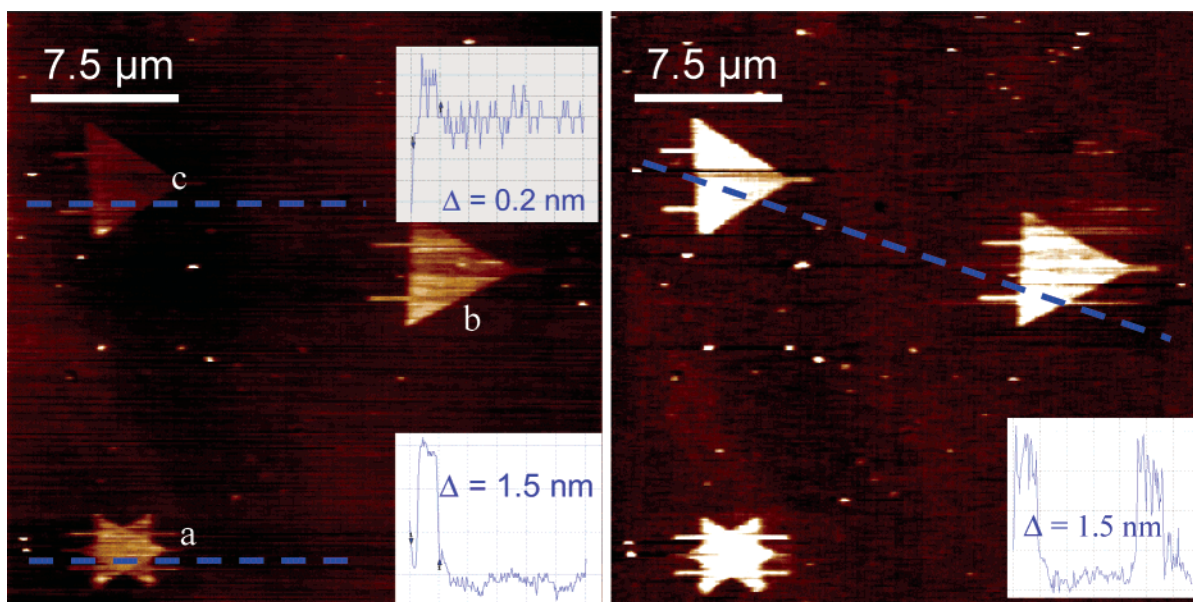


**Figure 9.** Contact-mode height images ( $30 \times 30 \mu\text{m}$ ) of the results of a sequential (six-step) buildup using oxidation and adhesion of TOA. Left image shows the results after five steps. Right image shows the results after the completion of six steps.

adsorption of gold particles onto surfaces opens routes toward further functionalization using, for example, well-known techniques from thiol chemistry. Functionalization of surfaces with optically active materials or proteins could create useful functional submicrometer-sized devices. Work in this direction is currently under investigation.

### Conclusions

We demonstrated the possibility to prepare and use submicrometer-sized patterns in subsequent functional-

ization reactions with quaternary ammonium salts and (functional) chlorosilanes, as well as cationic gold nanoparticles. The techniques for the binding of these molecules/particles to oxidized patterns are straightforward, and the obtained structures are stable against washing with solvents like water or toluene, also against cleaning with adhesive tape, and even during scanning in contact-mode AFM experiments. The functionalization of surfaces can also be done sequentially, thus opening routes for the specific adsorption/reaction of different functionalities onto

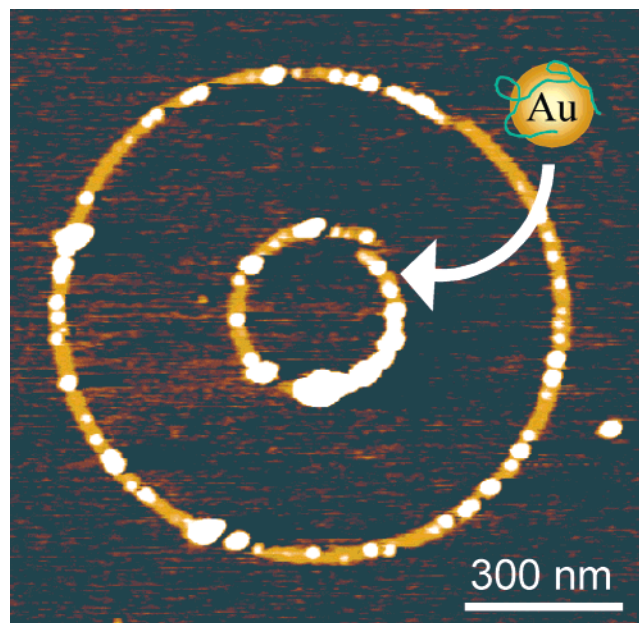


**Figure 10.** Tapping-mode height image ( $1.1 \times 1.1 \mu\text{m}$ ,  $z$  range = 18 nm) of cationic gold nanoparticles adsorbed to an oxidized structure. The observed height of the particles ranges from 17 to 20 nm.

a well-defined prepatterned surface. This was demonstrated by the six-step functionalization of a wafer with quaternary ammonium salts. Possible applications can be seen in fields like electronics as well as DNA and protein sensors. Currently, we are investigating the adsorbed cationic gold nanoparticles as starting points for the preparation of surfaces onto which proteins can be coupled through this coupling with the gold particles.

### Experimental Section

**Materials.** All reagents were used without further purification. OTS (95%) and BCH (99%) were obtained from Acros. UTS was obtained from ABCR. Toluene (Aldrich) was dried over sodium before use. Trimethyloctadecylammonium chloride (Aldrich) was dissolved in ultrapure water (resistivity 17.5 M $\Omega$ /cm). Cationic gold nanoparticles (20 nm) and unfunctionalized gold nanoparticles (40 nm) were obtained from BB-International. Silicon wafers (p-type, 7–21  $\Omega$ /cm) from WaferNet were obtained from Infineon.

**Instrumentation.** AFM experiments (both oxidation and imaging) were performed on NT-MDT Solver P47H and Solver LS7 machines. For optical images, a top-mounted optical microscope was available. For imaging, silicon tips (NSG10, 100  $\mu\text{m}$ , 255 kHz, NT-MDT) were used. For oxidation experiments, silicon tips with a coating of TiN or W<sub>2</sub>C (NSG01/TiN, CSG12/W<sub>2</sub>C NT-MDT) were utilized. The AFM sample stage consisted of a sapphire base plate with a metallic spring clip that allowed conductive connections to 1-cm<sup>2</sup> pieces of wafer. Wafers were oxidized in a UV–ozone photoreactor (UVP, PR-100). Contact-angle measurements were performed on a Krüss DSA10 system.

**Functionalization of the Wafers with OTS (See Figure 1a).** Small 1-cm<sup>2</sup> pieces of silicon wafer were oxidized in an ozone chamber for 15 min. The wafers were immersed in 0.03 mM OTS in BCH for 2 or 5 min, followed by thorough rinsing with toluene, leading to uniformly coated wafers with covalently attached silanes. If the reaction was carried out with toluene as the solvent, horizontally polymerized islands attached to the surface, which increased in size up to several micrometers with increasing reaction time. Complete functionalization was confirmed by contact-angle measurements.

**Patterning the Surface (See Figure 1b).** Oxidation of the surface was done in the contact mode under ambient conditions

(20–25 °C, relative humidity approximately 35–80%). For high-humidity conditions, oxidation patterns tend to be broader, and slightly less voltage ( $\sim 0.5$  V) needs to be applied. For both the stiff as well as the less-stiff tips (W<sub>2</sub>C,  $\sim 0.6$  N/m and TiN-coated,  $\sim 5$  N/m), the oxidations worked equally well. No deformation or oxidation was observed with too-low bias voltages, and the formation of deep oxidation features was observed at too-high bias voltages (1.5-nm deep, corresponding to the complete removal of the OTS monolayer). Only within a narrow range of conditions was oxidation without monolayer damage observed: bias voltage between  $-8$  and  $-10$  V, patterning speed around 3000 nm/s. The results of the oxidation depended highly on the tip quality; the W<sub>2</sub>C-coated tips have the advantage of being less stiff, thus reducing tip wear.

**Functionalization of the Patterns (See Figure 1c–e).** Functionalization of the inscribed patterns could in some cases be done on the AFM sample stage. In this case, the tip was briefly removed from the sample and a drop of liquid was placed on the sample. As a result of the hydrophobic nature of the wafer, the drop remained on the surface and could easily be removed by a filtration paper followed by rinsing with several drops of ultrapure water. This reaction procedure only worked in the case where no heating or prolonged reaction times were required. However, functionalization experiments with, for example, polymers could not be performed on the AFM sample stage, and the reactions were carried out in standard lab glassware. This allowed the usage of different solvents and better control over reaction parameters such as temperature and reaction atmosphere. To facilitate the retrieval of the area of interest after the reaction, the surface was marked by scratching the wafer with a scalpel close to the patterned area, and an image of the area was made with an optical microscope attached to the AFM microscope. Samples were not stirred to prevent the stirring bar from breaking the wafer.

**Chlorosilanes (See Figure 1c).** The terminal carboxylic acid groups on the oxidized areas were reacted with UTS by placing a 20-mmol solution in toluene on the wafer for 1–2 min. After reaction, the wafer was rinsed with toluene and water followed by cleaning with adhesive tape. 3M Office adhesive tape was found to be a good cleaning tool in general, not only for removing loosely bound particles but also for removing dust without damaging the structures even after multiple treatments.

**Polymer Grafting.** A polystyrene polymerization was done in the presence of an UTS functionalized surface. The wafer was immersed in a flask with styrene (10 g, 0.1 M) and azobisisobutyronitrile (3 mol %, 0.492 g, 0.03 M in toluene) at 90 °C for 24 h. To prevent the wafer from breaking, the contents were not stirred. After the reaction was stopped, the wafer was cleaned according to the earlier-mentioned procedure.

**Quaternary Ammonium Salts (See Figure 1d).** For the functionalization of surfaces with TOA, a drop of a 20-mmol solution in water was placed on the wafer for 15 min. The surface was cleaned with water and, if required, with adhesive tape. Cleaning was done by rinsing with ultrapure water. The sequential functionalization (Figure 7) of substrates was done by subsequently imaging, oxidizing, functionalizing, washing, and imaging the substrate. Adsorbed quaternary ammonium salts from initial steps were not removed by subsequent oxidation and washing.

**Cationic Gold Particles (See Figure 1e).** Cationic gold nanoparticles with a diameter of 20 nm were adsorbed by immersion of the patterned wafer in a 100-fold diluted water solution for 30 min, followed by rinsing in water and cleaning by adhesive tape. This procedure removed the particles that were loosely physisorbed but did not affect the particles adsorbed on the pattern.

**Acknowledgment.** The Dutch Polymer Institute (DPI) and the Fonds der Chemischen Industrie are acknowledged for the financial support. We thank Bart G. G. Kösters for helpful discussions and additional experiments.

LA034711X